Adsorption (2007) 13: 129–137
DOI 10.1007/s10450-007-9014-8

Adsorption of phenol by oil-palm-shell activated carbons

Aik Chong Lua · Qipeng Jia

Received: 14 December 2005 / Revised: 25 November 2006 / Accepted: 5 July 2007 / Published online: 6 September 2007

Abstract Steam activated carbons from oil-palm shells were prepared and used in the adsorption of phenol. The activated carbon had a well-developed mesopore structure which accounted for 45% of the total pore volume. The BET surface area of the activated carbon was 1183 m^2/g and a total pore volume of 0.69 cm^3/g using N_2 adsorption at 77 K. The adsorption capacity of the activated carbon for phenol was 319 mg/g of adsorbent at 298 K. The adsorption isotherms could be described by both the Langmuir-Freundlich and the Langmuir equations. The adsorption kinetics consisted of a rapid initial uptake phase, followed by a slow approach to equilibrium. A new multipore model is proposed that takes into account of a concentration dependent surface diffusion coefficient within the particle. This model is an improvement to the traditional branched pore model. The theoretical concentration versus time curve generated by the proposed model fitted the experimental data for phenol adsorption reasonably well. Phenol adsorption tests were also carried out on a commercial activated carbon known as Calgon OLC Plus 12 × 30 and the agreement between these adsorption data and the proposed model was equally good.

Keywords Activated carbon · Oil-palm shell · Phenol adsorption · Kinetic model · Surface diffusion

Abbreviations

a_L	Langmuir isotherm equation constant ($l \cdot mg^{-1}$)
b	Langmuir–Freundlich isotherm equation constant ($l \cdot mg^{-1}$)
c	Concentration in the aqueous phase ($mg \cdot l^{-1}$)
c_{eq}	Equilibrium aqueous phase concentration ($mg \cdot l^{-1}$)
c_o	Initial concentration in the aqueous phase ($mg \cdot l^{-1}$)
$C_{s,t}$	Aqueous phase concentration at particle surface at time t ($mg \cdot l^{-1}$)
C_t	Aqueous phase concentration at time t ($mg \cdot l^{-1}$)
D_{s0}	Effective surface diffusion coefficient at zero loading ($cm^2 \cdot s^{-1}$)
f	Fraction of the total adsorptive capacity utilized in mesopore
k	Correlation constant in kinetic model (dimensionless)
k_L	Langmuir isotherm equation constant ($l \cdot g^{-1}$)
K	Freundlich isotherm equation constant $(mg \cdot g^{-1})(l \cdot mg^{-1})^{n_F}$
K_b	Branched pore rate coefficient, s^{-1}
K_f	External aqueous phase mass transfer coefficient ($cm \cdot s^{-1}$)
m	Weight of the adsorbent (g)
$\dot{m}_b$	Mass transfer rate of adsorbate from mesopore region to micropore region ($g \cdot s^{-1}$)
n_F	Freundlich isotherm equation constant (dimensionless)
N	Rotational speed of orbital shaker (rpm)
N_{pt}	Number of points on a fitted experimental curve (dimensionless)
n_s	Three-parameter isotherm equation constant (dimensionless)
q	Adsorption capacity ($mg \cdot g^{-1}$)
q_{av}	Amount adsorbed on the adsorbent ($mg \cdot g^{-1}$)
q_b	Solid phase concentration in micropore region ($mg \cdot g^{-1}$)
q_{eq}	Equilibrium solid phase concentration ($mg \cdot g^{-1}$)

A.C. Lua (✉) · Q. Jia
School of Mechanical and Aerospace Engineering, Nanyang Technological University, 50 Nanyang Avenue, Singapore 639798, Republic of Singapore
e-mail: maclua@ntu.edu.sg

q_m Solid phase concentration in mesopore region ($mg \cdot g^{-1}$)
q_{msat} Adsorbate concentration in mesopore at surface saturation ($mg \cdot g^{-1}$)
Q Three parameter isotherm equation constant ($mg \cdot g^{-1}$)
r Radial distance from centre of particle (cm)
R Particle radius (cm); Gas constant ($kJ \cdot kg^{-1} \cdot K^{-1}$)
T Absolute temperature (K)
V_f Solution volume (l)
ΔH^0 Standard enthalpy change during adsorption ($kJ \cdot kg^{-1}$)
ΔS^0 Standard entropy change during adsorption ($kJ \cdot kg^{-1} \cdot K^{-1}$)

Greek letters

ρ Adsorbent particle density, ($g \cdot ml^{-1}$)
ψ Proportionality factor defined in van't Hoff equation (dimensionless)

1 Introduction

The occurrence of various organic chemicals in hydrosphere presents a major problem in the usage of water resources. Hydroxybenzene or phenol and its analogous, recognized priority pollutants, enter into the environment through numerous chemical industries, viz., coal conversion, petroleum refining, textile, pharmaceutical, timber, mining, paper and pulp, as well as large-scale use of herbicides, insecticides and pesticides in agriculture (Report 1998). Phenols are also released as intermediate products during microbial degradation of pesticides or some other xenobiotics (Hottenstein et al. 1995). Complete removal of these carcinogenic compounds or in some cases reduction of the load of such solutes to an acceptable concentration has become a major challenge to preserve the quality of aquatic life. The promising options for the treatment of phenolic wastes are through biological, chemical and physical methods. Although biological method for detoxification using different microorganisms is feasible, it is only applicable for the low concentration range. Conventional physical and chemical methods for removal or transformation of phenolic wastes include adsorption, ion exchange and membrane processes. Selection and feasibility of a particular operation are based on its application to the solute concentration range, capacity, cost, reusability and reproducibility (Buchanan and Nicell 1995; Karamanev et al. 1997).

In adsorption, the kinetics between the individual atoms, ions or molecules of an adsorbate and the surface or interface are dependent on the forces and the various interactions. Equilibrium studies can provide fundamental information to model the adsorption of an adsorbate onto an adsorbent. In the adsorption of phenol, which has large molecules and a long contact time to equilibrium, the adsorption mechanism is likely to be diffusion control. Diffusion adsorption is usually controlled by an external film resistance and/or internal diffusion mass transport or intraparticle diffusion. Ko et al. (2002, 2003) and Yang and Al-Duri (2001) studied the branched pore diffusion model (BPDM) and applied it to the single component adsorption of dyes on activated carbon in batch stirred vessels. They studied the diffusion coefficients within the particle which varied with the solute concentration. Yang and Al-Duri (2001) proposed that the surface diffusion coefficient could be successfully described as an exponential function of the surface coverage. Incorporating this surface diffusion coefficient, this paper proposes a new concentration dependent effective surface diffusion coefficient into the branched pore model to relate the sorbent surface, the solute properties and the adsorptive characteristics. A branched pore kinetic model or multi-pore for aqueous phase activated carbon adsorption is presented in which the carbon particle is partitioned into rapidly and slowly diffusing regions. This proposed model overcomes problems arising from a single rate parameter analysis and therefore should provide better agreement with experimental data.

2 Adsorption isotherms

Adsorption isotherms are important to relate the mechanics in which the adsorbates will interact with the adsorbents. The Langmuir equation, the empirical Freundlich equation and the three parameter Langmuir–Freundlich equations are used to characterize the adsorption isotherms of activated carbons.

The Langmuir isotherm equation is

$$q_{eq} = \frac{k_L c_{eq}}{1 + a_L c_{eq}} \tag{1}$$

where c_{eq} and q_{eq} are the concentrations in the aqueous and solid phases, respectively, at equilibrium, and k_L and a_L are constants that correspond to monolayer coverage.

The Freundlich isotherm equation is

$$q_{eq} = K c_{eq}^{1/n_F} \tag{2}$$

where K and n_F are constants for a given solid liquid adsorption system. K is widely used to quantify the extent of adsorption and to provide an easy way to compare different adsorbents or conditions for a particular system.

The three-parameter Langmuir–Freundlich isotherm equation is

$$q_{eq} = Q \frac{b c_{eq}^{1/n_s}}{1 + b c_{eq}^{1/n_s}} \tag{3}$$

where Q, b and n_s are constants for a given liquid adsorption system. The Langmuir–Freundlich model was analyzed

by Sips (1948) who found that the energy distribution function corresponded to a symmetrical quasi-Gaussian function. At low concentrations, the model reduces to the Freundlich model and in the case of an homogeneous surface, it reduces to the Langmuir model (Quinones and Guiochon 1998).

Since the Langmuir–Freundlich model has more than two adjustable parameters, it is necessary to apply nonlinear least-squares analysis. In order to compare the validity of the three isotherm equations quantitatively, the normalized and non-normalized RMS (root mean square) residuals were computed and were used as criteria for determining the effectiveness of a particular model to fit the adsorption isotherm data. The usage of these two criteria is based on the calculation of errors. For nonnormalized RMS residual, it is more sensitive to errors at high equilibrium solution concentrations as it weighs the actual error at all points. However, the normalized RMS residual is based on the relative error and therefore it weighs all points equally. The formulae of the normalized RMS and the nonnormalized RMS residuals are

Normalized RMS (NRMS) residual

$$= 100 \times \sqrt{\frac{1}{N_{pt}} \cdot \sum_{i=1}^{N_{pt}} \left(\frac{q_{e,i(\exp)} - q_{e,i(calc)}}{q_{e,i(\exp)}} \right)^2} \tag{4}$$

Nonnormalized RMS (NNRMS) residual

$$= \sqrt{\frac{1}{N_{pt}} \cdot \sum_{i=1}^{N_{pt}} (q_{e,i(\exp)} - q_{e,i(calc)})^2}. \tag{5}$$

3 Kinetic adsorption model

The governing equations of the proposed concentration dependent branched pore kinetic model are as follows.

1. The macroscopic mass conservation equation of the adsorbate in the aqueous phase is

$$\mathrm{V}_f \frac{dC_t}{dt} = -\mathrm{m} \frac{dq_{av}}{dt} \tag{6}$$

where m is the mass of the adsorbent, V_f is the solution volume and C_t is the aqueous phase concentration at time t. The amount adsorbed in the solid phase, q_{av}, is given by:

$$q_{av} = \frac{3}{\mathrm{R}^3} \int_0^{\mathrm{R}} [f q_m + (1-f) q_b] r^2 dr \tag{7}$$

where f is the part of the total adsorptive capacity utilized in the mesopore, q_m and q_b are the solid phase concentrations in the mesopore and micropore regions respectively, R is the adsorbent particle radius, and r is the radial distance from the centre of the adsorbent particle.

2. The mesopore mass balance equation is

$$\mathrm{f} \frac{\partial q_m}{\partial t} + (1-\mathrm{f}) \frac{\partial q_b}{\partial t} = \frac{\mathrm{f} D_{s0}}{r^2} \frac{\partial}{\partial r} \left(r^2 \exp\{\mathrm{k}(q_m/\mathrm{q_{msat}})\} \frac{\partial q_m}{\partial r} \right) \tag{8}$$

where $\mathrm{D_{s0}}$ is the effective surface diffusion coefficient at zero loading, q_{msat} is the adsorbate concentration in the mesopore region at surface saturation, and k is a constant.

3. The micropore mass balance equation is

$$(1-\mathrm{f}) \frac{\partial q_b}{\partial t} = \mathrm{K}_b (q_m - q_b) = \dot{m}_b \tag{9}$$

where K_b is the branched pore rate coefficient, and $\dot{m}_b$ is the rate of mass transfer of adsorbate from mesopore region to micropore region.

4. The coupling between the aqueous and solid phases achieved by equating the fluxes at the solid-aqueous interface is

$$\mathrm{K}_f (C_t - C_{s,t}) = \mathrm{f} D_{s0} \exp\{k(q_m/\mathrm{q_{msat}})\} \rho \left(\frac{\partial q_m}{\partial r} \right)_{r=\mathrm{R}} \tag{10}$$

where K_f is the external aqueous phase mass transfer coefficient, $C_{s,t}$ is the aqueous phase concentration at the particle surface at time, t, and ρ is the solid density of the adsorbent.

5. The Langmuir isotherm as given in (1) is used for the local equilibrium at the interface between the aqueous and the adsorbent solid phases.

The following boundary and initial conditions are

$$q_m(r,0) = 0 \tag{11}$$

$$q_b(r,0) = 0 \tag{12}$$

$$C_t(t=0) = \mathrm{C}_0 \tag{13}$$

$$q_m(\mathrm{R},t) = q_s(t) \tag{14}$$

$$\frac{\partial q_m}{\partial r}(0,t) = 0. \tag{15}$$

The method of orthogonal collocations (Do 1998) was used to solve this model.

4 Adsorption enthalpy

The adsorption enthalpy can be obtained from the van't Hoff equation which is

$$\ln(q_{eq}/c_{eq}) = -\frac{\Delta H^0}{\mathrm{RT}} + \left(\frac{\Delta S^0}{\mathrm{R}} - \ln \psi \right) \tag{16}$$

where R is the gas constant, T is the temperature of the adsorption system, ΔH^0 and ΔS^0 are the enthalpy change and entropy change during adsorption, respectively, and ψ is the proportionality factor. If ΔH^0, ΔS^0 and ψ are constant, a plot of $\ln(\frac{q_{eq}}{c_{eq}})$ versus $\frac{1}{T}$ will yield a straight line with a slope of $-\Delta H^0/\mathrm{R}$ and hence ΔH^0 can be calculated.

5 Experimental

The raw oil-palm shells were crushed and sieved to a size range of 2–2.8 mm. After drying at 383 K in an electrical oven for 24 hours, the shells were placed in a vertical stainless steel reactor and heated under vacuum from room temperature to 673 K at a heating rate of 10 K/min. The sample was held at the final temperature for 2 hours during pyrolysis. Subsequently, the resulting chars were removed and placed into another reactor for activation. The chars were heated under nitrogen atmosphere from room temperature to 1173 K at a heating rate of 10 K/min. Having reached the final temperature of 1173 K, steam from an electric steam generator was introduced. The hold time during steam activation was 1 hour. The resulting activated carbons were characterized using an accelerated surface area and porosimetry system (ASAP 2010, Micromeritics) under N_2 adsorption at 77 K. Using the Brunauer-Emmett-Teller (BET) equation, data from the isotherms were used to determine the BET surface area (Gregg and Sing 1982). The Dubinin-Radushkevich equation was used to calculate the micropore volume (Dubinin 1975). The total pore volume was estimated to be the liquid volume of adsorbate (N_2) at a relative pressure of 0.985. The difference between the total pore volume and the micropore volume is the mesopore volume. The pore size distribution of the activated carbon was obtained by applying the density functional theory on the N_2 adsorption isotherm data.

The adsorbate used in the activated carbon adsorption studies was Phenol GR which was supplied by Merck & Co. The equilibrium adsorption capacities of the activated carbons for phenol at various initial adsorbate concentrations were measured to determine the adsorption isotherms for phenol. The aqueous phase adsorption studies were carried out at five different temperatures of 298 K, 303 K, 313 K, 318 K and 323 K. For each temperature, five different solution concentrations were studied. 50 ml of each solution was poured into a 125 ml conical flask. An accurately weighed amount of activated carbon was added into each flask. The activated carbons were washed with boiling deionized water and subsequently dried at 110 °C for 24 hours before use. An additional flask with a known phenol solution, but without any activated carbon, was used as the control experiment. By verifying that the initial and final concentration of this control flask remaining the same, phenol loss through volatilization and adsorption onto the walls of the flask was negligible. All the six flasks were placed in a shaker bath (DK-SB020, Daiki) operating at 900 degrees per second for 168 hours. By determining the phenol solution concentration before and after the adsorption test, the amount of phenol adsorbed by the activated carbons could be found. The phenol concentration was determined by a gas chromatograph-mass spectrometer (6890N GC-5973MSD system, Agilent).

To study the adsorption kinetics with time, the adsorption of phenol by the oil-palm-shell activated carbons was carried out in a batch process. In particular, the effect of the initial solution concentration on the rate of phenol adsorption was investigated. An accurate weighed amount of activated carbon was added to 50 cm^3 of phenol solution in a 100 cm^3 conical flask. The flask was then agitated in a thermostatic orbital shaker at a temperature of 323 K and a rotational speed of 900 degrees per second over a period of 6 days. Two initial phenol concentrations were studied; the other operating parameters remaining constant. The phenol concentration was determined by the same gas chromatograph-mass spectrometer mentioned earlier. The technique used was based on the EPA method 8720. The amount of phenol adsorbed was determined by the mass balance procedure.

A commercial activated carbon, Calgon OLC Plus 12 × 30, produced by Calgon Carbon Corp. was evaluated for its phenol adsorption characteristics so that a comparative analysis between the oil-palm-shell activated carbon in this study and a commercial activated carbon could be made. The Calgon activated carbon was also characterized by the ASAP 2010 system using nitrogen adsorption at 77 K to determine its BET surface area, micropore volume and total pore volume. Phenol adsorption isotherms and adsorption kinetics with time for this commercial carbon were similarly studied at an adsorption temperature of 323 K.

6 Results and discussion

Figure 1 shows the nitrogen adsorption isotherm at 77 K for the steam activated carbon prepared from oil-palm shell. For the micropore analysis in the ASAP 2010 system, N_2 adsorption isotherm was obtained in the very low pressure region for a range of relative pressures between 3×10^{-6} and 0.1. In the mesopore analysis, normal N_2 adsorption was carried out at relative pressures from 0.06 to 0.985. The isotherm in Fig. 1 belongs to a mixed of Type I isotherm which is associated with microporous solid having a relatively small external surface area, and Type IV isotherm which is associated with mesoporous structures. In accordance to the classification adopted by the International Union of Pure and Applied Chemistry (IUPAC), pores are classified as micropores (<2 nm diameter), mesopores (2–50 nm diameter) and macropores (>50 nm diameter).

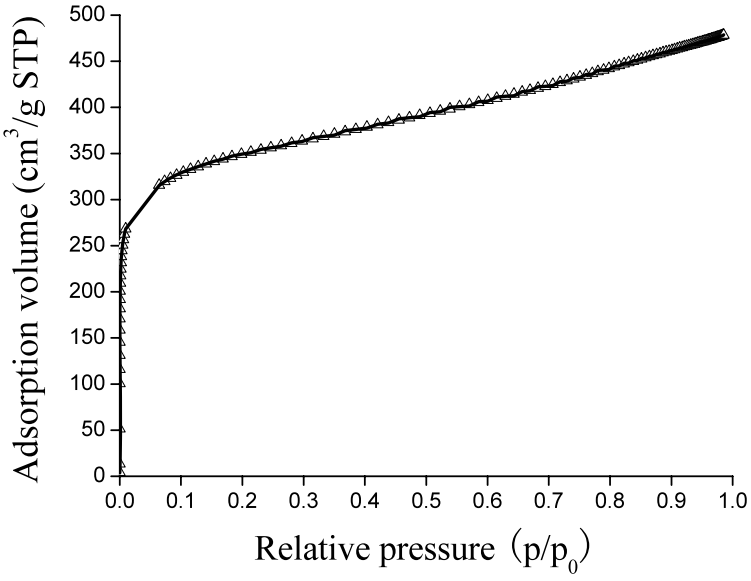

Fig. 1 Nitrogen adsorption isotherm of the activated carbon prepared from oil-palm shell

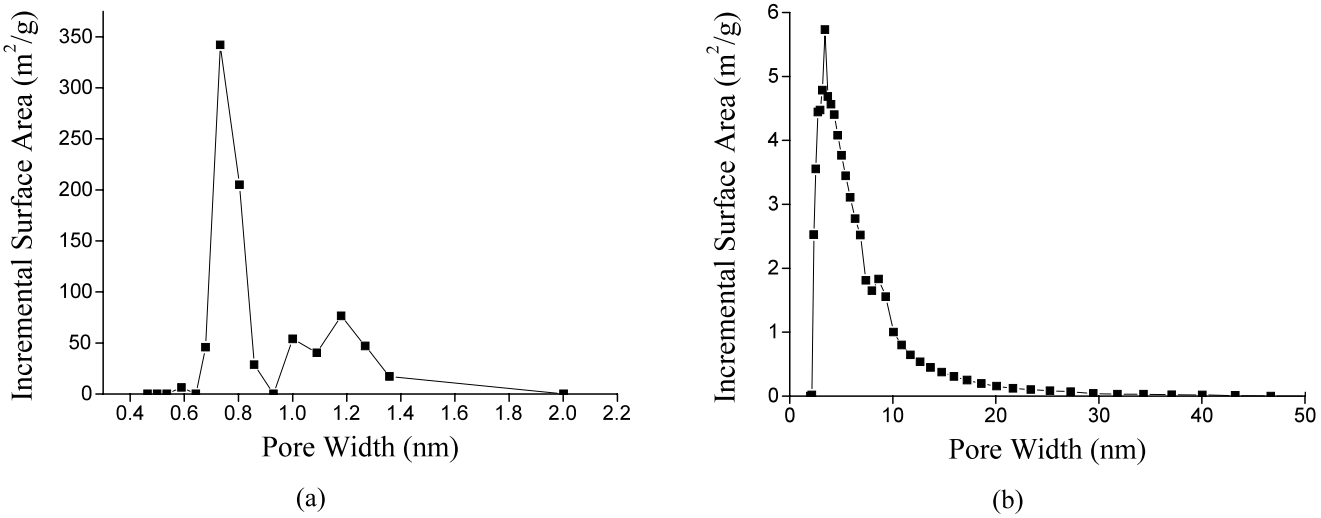

Fig. 2 (**a**) Micropore, and (**b**) mesopore size distributions of activated carbons prepared from oil-palm shells

Based on this classification, aqueous-phase activated carbons should consist predominantly of mesopores. The pore size distribution of the activated carbon was obtained from the nitrogen adsorption isotherm in Fig. 1 using the density functional theory. Figure 2a shows the micropore size distribution of the activated carbon based on the micropore analysis in the low pressure region whilst Fig. 2b depicts the mesopore size distribution based on the normal pore analysis in the ASAP 2010 system. Figure 2 confirms that the activated carbon consists of micro-mesopores with dominant pore sizes of 0.8 and 3.4 nm for the micropore and mesopore size ranges, respectively. With these pore sizes, the oil-palm-shell activated carbons developed in this work are well suited for the phenol adsorption studies.

Table 1 shows the physical properties of both activated carbons that were used in the adsorption tests. With average pore diameters of 2.33 and 1.92 nm for the oil-palm-shell and Calgon activated carbons respectively, and relatively significant proportion of mesopores, both activated carbons are suitable for aqueous phase adsorption such as the phenol adsorption tests described in this study. These two activated carbons have almost similar physical characteristics and are therefore well suited for the comparison of phenol adsorption between them.

The adsorption isotherms of phenol onto the oil-palm-shell activated carbons at various solution temperatures are shown in Fig. 3. The largest adsorption capacity shown was 319 mg phenol/g adsorbent at a solution temperature of 298 K. The adsorption curves fitted from the Langmuir,

Table 1 Surface characterization of the activated carbons

Type of activated carbon	BET surface area (m^2/g)	Total pore volume (cm^3/g)	Average pore diameter (nm)	Proportion of mesopore volume to total pore volume (%)
Oil-palm shell	1183	0.69	2.33	45
Calgon	1113	0.54	1.92	39

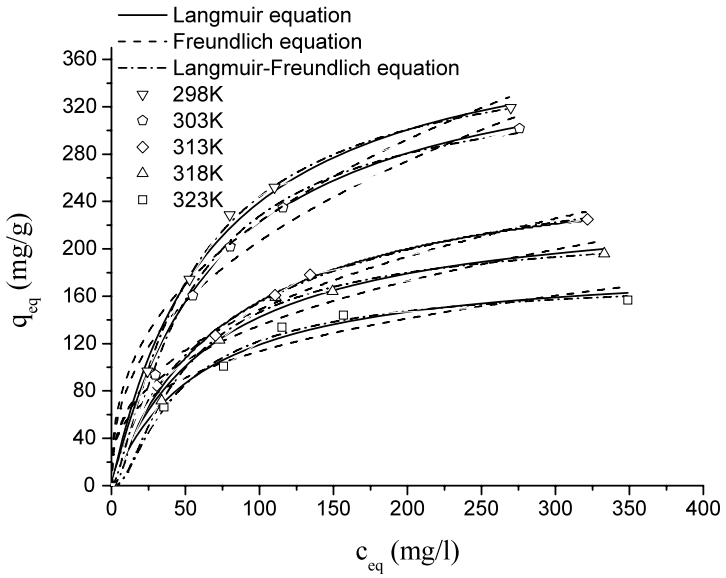

Fig. 3 Phenol adsorption isotherms at various temperatures and their correlations to Langmuir, Freundlich and Langmuir–Freundlich equations for oil-palm-shell activated carbons

Table 2 Adsorption parameters derived from Langmuir, Freundlich and Langmuir–Freundlich equations for various adsorption temperatures for oil-palm-shell activated carbons

Temperature	Langmuir				Freundlich				Langmuir–Freundlich				
(K)	k_L (mg/g)	a_L (l/mg)	NRMS (%)	NNRMS	K (mg/g)(l/mg)^{n_F}	$1/n_F$	NRMS (%)	NNRMS	Q (mg/g)	b (l/mg)	$1/n_s$	NRMS (%)	NNRMS
298	5.90	0.015	4.77	6.73	36.88	0.39	15.74	20.33	418.60	0.022	0.89	1.78	3.13
303	5.22	0.014	9.10	10.08	31.41	0.41	16.36	18.44	381.90	0.016	0.97	2.90	4.12
313	3.50	0.013	2.53	2.79	26.90	0.38	5.50	6.40	321.10	0.020	0.82	1.34	1.50
318	3.46	0.014	5.64	6.12	26.42	0.35	14.31	13.96	251.78	0.019	0.92	5.06	6.01
323	3.17	0.017	5.28	6.17	26.63	0.26	12.67	12.46	185.60	0.024	0.94	4.72	5.17

the Freundlich and the Langmuir–Freundlich equations are also shown in the figure. Generally, increasing solution temperature decreases the adsorption capacity of the adsorbent and hence the equilibrium solid phase concentration decreases. This is to be expected due to the exothermic effect of adsorption; the molecular motions of the adsorbate molecules increase with temperature and thereby reduce the sorption of these molecules onto the pore surfaces. The adsorption capacity of the oil-palm-shell activated carbons decreased from 319 (initial solution concentration of 270 mg/l) to 157 mg phenol/g activated carbon (initial solution concentration of 349 mg/l) when the solution temperature increased from 298 to 323 K, respectively. The Langmuir and the Langmuir–Freundlich curves provide good agreement with the experimental adsorption data for the whole range of solution concentrations while the Freundlich curve resulted in reduced agreement with the experimental data. Table 2 shows the adsorption parameters as obtained from the three isotherm equations for the oil-palm-shell activated carbons using various adsorption temperatures. As the adsorption capacity decreases with increasing solution temperature, the constants k_L, K and Q, which quantify the extent of adsorption, in the Langmuir, Freundlich and Langmuir–Freundlich equations respectively, also generally decrease with increas-

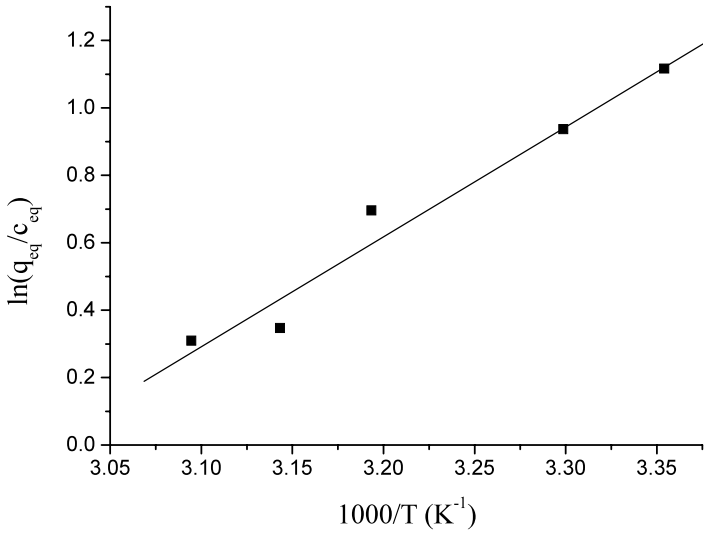

Fig. 4 Plot of $\ln(\frac{q_{eq}}{c_{eq}})$ versus $\frac{1000}{\mathrm{T}}$

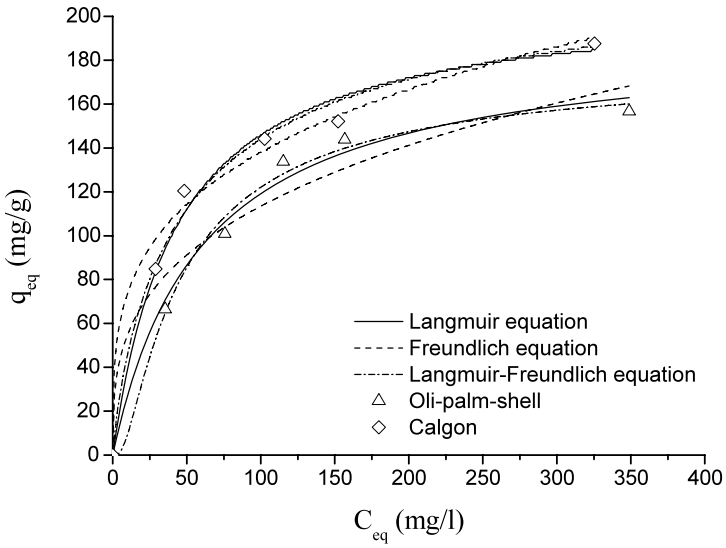

Fig. 5 Phenol adsorption isotherms at 323 K for the two types of activated carbons and their correlations to Langmuir, Freundlich and Langmuir–Freundlich equations

ing temperature. The other constants, namely, a_L, n_F, b and n_s, in the three isotherm equations do not generally fluctuate appreciably with different solution temperatures. The data for the error residuals also confirm the Langmuir and the Langmuir–Freundlich equations provide better agreement for the experimental data points than the Freundlich equation.

Figure 4 shows the plot of $\ln(\frac{q_{eq}}{c_{eq}})$ versus $\frac{1000}{\mathrm{T}}$ for five different solution temperatures. The data are extracted from the five phenol adsorption isotherms given in Fig. 3. A linear relationship is obtained, in which the slope is $-\frac{\Delta H^0}{\mathrm{R}}$. Hence, an average enthalpy change of -27 kJ/mol was obtained for all the adsorption tests presented in Fig. 3. The negative value for ΔH^0 indicates that the phenol adsorption is an exothermic process. This value of enthalpy change is in good agreement with the absolute value of 25 kJ/mol obtained by Salvador and Merchan (1996) for the adsorption of phenol from an aqueous solution by a typical activated carbon.

Figure 5 shows the phenol adsorption isotherms for both oil-palm-shell and Calgon activated carbons at a solution temperature of 323 K. The adsorption isotherms using Langmuir, Freundlich and Langmuir–Freundlich equations are also plotted. Similar to Fig. 3, the Langmuir and Langmuir–Freundlich equations also show good agreement with the experimental adsorption data for the Calgon activated carbon. Table 3 lists the equilibrium adsorption parameters for both activated carbons. The Calgon activated carbon exhibits slightly better phenol adsorption capacity than the oil-palm-shell activated carbon as shown in Fig. 5 and Table 3 which shows higher values of k_L, K and Q for the Calgon activated carbon.

The experimental data for the adsorption kinetic study for two phenol solutions of 38 and 117 mg/l using the oil-palm-shell activated carbons are shown in Fig. 6. Using a phe-

Table 3 Adsorption parameters derived from Langmuir, Freundlich and Langmuir–Freundlich equations for oil-palm-shell and Calgon activated carbons at 323 K

Type of activated carbon	Langmuir				Freundlich				Langmuir–Freundlich				
	k_L (mg/g)	a_L (l/mg)	NRMS (%)	NNRMS	K (mg/g)(l/mg)^{n_F}	$1/n_F$	NRMS (%)	NNRMS	Q (mg/g)	b (l/mg)	$1/n_s$	NRMS (%)	NNRMS
Oil-palm shell	3.17	0.017	5.28	6.17	26.63	0.26	12.67	12.46	185.60	0.024	0.94	4.72	5.17
Calgon	4.82	0.023	5.10	7.41	39.40	0.27	8.70	9.46	225.13	0.037	0.84	5.41	7.25

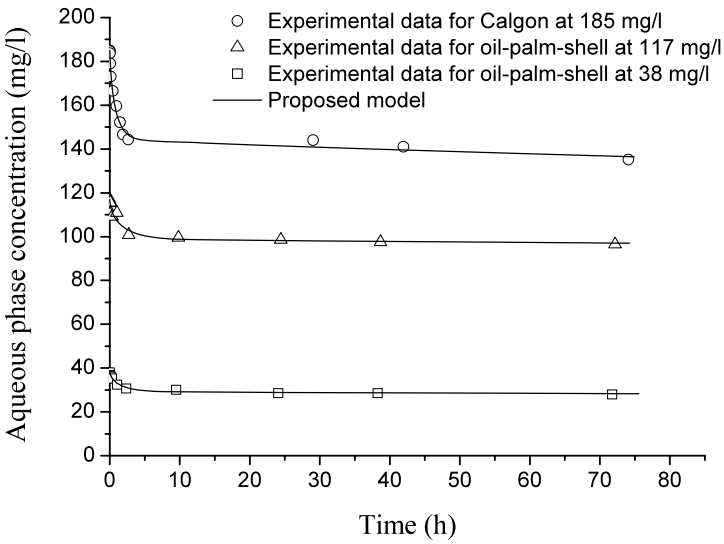

Fig. 6 Correlation between experimental adsorption data at 323 K and proposed model for the two types of activated carbons

Table 4 Fitted parameters as obtained by the nonlinear regression of the adsorption rate data at 323 K

Type of activated carbon	c_o (mg/l)	m (mg)	N (rpm)	K_f (cm/s)	D_{s0} (cm^2/s)	K_b (s^{-1})	f	k	Correlation coefficient
Calgon	185	14.46	150	$3.06e^{-1}$	$1.13e^{-7}$	$6.70e^{-7}$	0.89	0.37	0.98
Oil-palm shell	117	11.32	150	$3.94e^{-1}$	$4.12e^{-8}$	$2.99e^{-7}$	0.69	0.69	0.96
Oil-palm shell	38	10.04	150	$3.87e^{-1}$	$7.19e^{-8}$	$3.58e^{-7}$	0.71	0.49	0.98

nol solution of 185 mg/l, the kinetic adsorption data for the Calgon activated carbon is also shown in Fig. 6. The steep initial drop of the solute concentration is to be expected as the adsorption rate is high for an unloaded adsorbent. The data from these three experimental tests were regressed using the proposed concentration dependent branched pore kinetic model in a nonlinear least squares routine and the theoretical curves were also plotted in Fig. 6. The agreement between the experimental data and the model is good. The fitted parameters using the proposed model are given in Table 4. The calculated values of D_{s0} and K_b given in Table 4 are less than that for K_f; this indicates that the rate controlling factor is the effective diffusion within the pore structure of the adsorbent particle. The values of the parameter k are not negligible and therefore show that the surface diffusion coefficient is dependent on the solid phase adsorbate concentration. The good agreement, with correlation coefficients of at least 0.96, between the kinetic simulations and the experimental results for two different activated carbons verifies that the proposed model is accurate for predicting the adsorption kinetics in aqueous solutions and the lumped parameter approach for the micropore transport appears to be quite effective for describing the adsorptive behaviour.

7 Conclusions

1. Activated carbons were prepared from oil-palm shells by pyrolysis under vacuum and subsequently the resulting chars were activated using steam. The adsorption isotherms of the activated carbons belonged to a mixed Type I and Type IV isotherms. Therefore, the pores of the carbons consisted of both microporous and mesoporous structures. The activated carbons had well developed

pore structures with a BET surface area of 1183 $m^2\,g^{-1}$, a total pore volume of a 0.69 $cm^3\,g^{-1}$ and the percentage of mesopore volume to total pore volume of 45%. These microporous-mesoporous activated carbons are suitable for aqueous phase adsorption. The largest adsorption capacity was 319 mg phenol/g adsorbent at 298 K in a batch process.

2. The phenol adsorption capacity of the activated carbon is a function of the solution temperature. Increasing solution temperature increases the kinetic motion of the adsorbate molecules and therefore diminishes their sorption onto the pore surfaces. The adsorption capacity of the oil-palm-shell activated carbons decreased from 319 (initial solution concentration of 270 mg/l) to 157 mg phenol/g activated carbon (initial solution concentration of 349 mg/l) when the solution temperature increased from 298 to 323 K, respectively.
3. Both the Langmuir equation and the three-parameter Langmuir–Freundlich equation show good agreement with the adsorption isotherm data for the oil-palm-shell activated carbons over a range of solution temperatures of 298 to 303 K. The overall enthalpy change of the adsorption process based on the oil-palm-shell activated carbons was −27 kJ/mol, indicating that adsorption is an exothermic process. These two equations also provided good agreement with the adsorption data for the Calgon activated carbon.
4. A concentration dependent branched pore kinetic model is proposed in which a concentration dependent surface diffusion coefficient within the adsorbent particle is considered. The good agreement between the kinetic adsorption data for two different activated carbons (oil-palm-shell and Calgon activated carbons) and the model is indicative that the model is effective for aqueous phase adsorption rate predictions.

References

Buchanan, I.D., Nicell, J.A.: Model development for horseradish peroxidase catalyzed removal of aqueous phenol. Biotechnol. Bioeng. **54**, 251–261 (1995)

Do, D.D.: Adsorption Analysis: Equilibria and Kinetics. Imperial College Press, London (1998)

Dubinin, M.M.: In: Cadenhead, D.A. (ed.) Progress in Surface and Membrane Science, vol. 9, p. 25. Academic, New York (1975)

Gregg, S.J., Sing, K.S.W.: Adsorption, Surface Area, and Porosity. Academic, London (1982)

Hottenstein, C.S., Jourdan, S.W., Hayes, M.C., Rubio, F.M., Herzog, D.P., Lawruk, T.S.: Determination of pentachlorophenol in water and soil by a magnetic particle-based enzyme immunoassay. Environ. Sci. Technol. **29**, 2754–2758 (1995)

Karamanev, D.G., Chavarie, C., Samson, R.: Soil immobilization: New concept for biotreatment of soil contaminants. Biotechnol. Bioeng. **57**, 471–476 (1997)

Ko, D.C.K., Porter, J.F., McKay, G.: A branched pore model analysis for the adsorption of acid dyes on activated carbon. Adsorption **8**, 171–188 (2002)

Ko, D.C.K., Tsang, D.H.K., Porter, J.F., McKay, G.: Applications of multipore model for the mechanism identification during the adsorption of dye on activated carbon and bagasse pith. Langmuir **19**, 722–730 (2003)

Quinones, I., Guiochon, G.: Extension of a Jovanovic-Freundlich isotherm model to multicomponent adsorption on heterogeneous surfaces. J. Chromatogr. A **796**, 15–40 (1998)

Salvador, F., Merchan, M.D.: Study of the desorption of phenol and phenolic compounds from activated carbon by liquid-phase temperature-programmed desorption. Carbon **34**, 1543–1551 (1996)

Sips, R.: On the structure of a catalyst surface. J. Chem. Phys. **16**, 490–495 (1948)

Toxicological Profile for Chlorophenols, Report of US Department of Health and Human Services (1998)

Yang, X.Y., Al-Duri, B.: Application of branched pore diffusion model in the adsorption of reactive dyes on activated carbon. Chem. Eng. J. **83**, 15–23 (2001)